Catalysis Letters
https://doi.org/10.1007/s10562-020-03340-7

Tuning Microenvironment of Quaternary Ammonium Salt and Tertiary Amine Bifunctionalized Polyacrylonitrile Fiber for Cooperatively Catalyzed Aza-Michael Addition

Xueyu Yuan[1] · Huimin Du[1] · Jingyan Zhao[1] · Anyaegbu Ejike Chima[1] · Ning Ma[1,2] · Minli Tao[1,3] · Wenqin Zhang[1,2]

Received: 6 June 2020 / Accepted: 26 July 2020

Abstract

A series of novel polyacrylonitrile fiber catalysts modified with different ratio of quaternary ammonium salt (QA) to tertiary amine (TA) were screened for heterogeneously catalyzed aza-Michael addition in water. The best catalyst was found to be $\mathrm{PAN_{PQ\text{-}1}F}$ with a QA:TA ratio of 1:1, which can lead to high yield, excellent selectivity of solvent and great recyclability under optimized conditions. The special microenvironment of hydrophilic inner layer and hydrophobic surface layer of $\mathrm{PAN_{PQ\text{-}1}F}$ is conducive to the leaving of the product and the high conversion of the reaction. Based on the fact that appropriate microenvironment combined with the catalytic sites promoted the reaction, cooperative effect of QA and TA in the microenvironment of $\mathrm{PAN_{PQ\text{-}1}F}$ catalyst was proposed.

Graphic Abstract

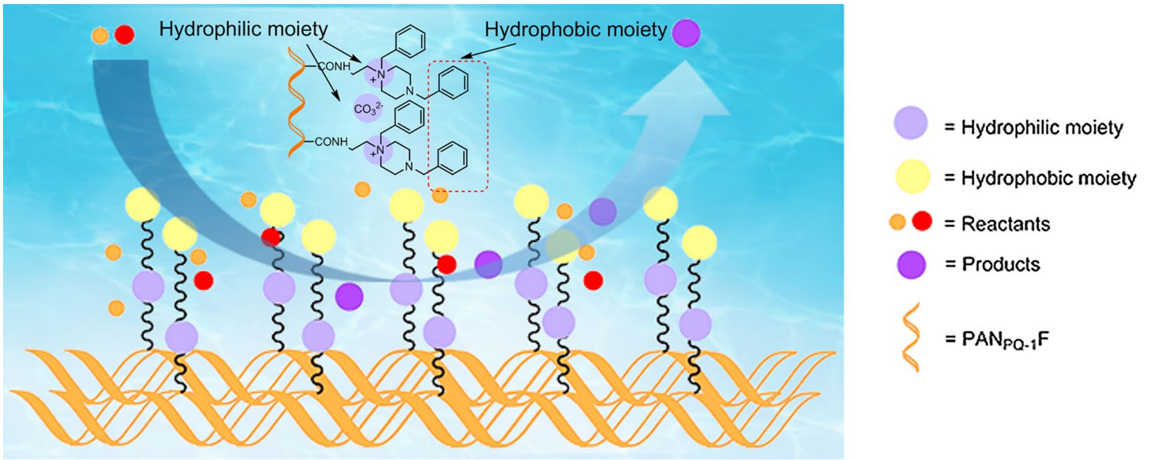

Keywords Polyacrylonitrile fiber · Cooperative catalysis · Microenvironment · Aza-michael addition

---

Electronic supplementary material The online version of this article (https://doi.org/10.1007/s10562-020-03340-7) contains supplementary material, which is available to authorized users.

✉ Ning Ma
mntju@tju.edu.cn

[1] Department of Chemistry, School of Sciences, Tianjin University, Tianjin 300072, People's Republic of China

[2] Collaborative Innovation Center of Chemical Science and Engineering (Tianjin), Tianjin 300072, People's Republic of China

[3] National Demonstration Center for Experimental Chemistry & Chemical Engineering Education, Tianjin University, Tianjin 300350, China

1 Introduction

For green chemical production, the recycling of catalysts is of great importance. Recently, there have been examples of highly efficient small-molecule catalysts grafted covalently onto solid supports, such as silica [1, 2], zeolites [3, 4], metal oxides [5, 6], polymers [7, 8], and metal–organic frameworks [9–11]. In this way, the state-of-the-art heterogeneous catalysts showed the advantages of easy separation and outstanding recovery capacity [12]. Because water is non-toxic, low-cost and easily available, it's widely regarded as a green solvent [13]. However, many heterogeneous catalysts hardly perform well in aqueous media. For example, one of the drawback of zeolites is their sensitivity to hot water, which may hinder their full utilization in aqueous phase reactions [14, 15]. The organic phase in aqueous solution is difficult to enter into the pores of some mesoporous materials [16], which leads to the decrease of catalytic efficiency. Therefore, development of new support materials to overcome this drawback is important for green chemical production in both industry and academia.

The tuning of microenvironment near the catalytic sites have been comprehensively proved to dramatically enhance the activity of a catalyst [17, 18]. For heterogeneous catalysis in water, the mass transfer resistance between aqueous and organic phases is also crucial [19–21]. Therefore, the hydrophilicity/hydrophobicity near the catalytic sites can be regulated to improve the catalytic activity [22]. For example, a series of mesoporous silica catalysts with different wettability have been prepared by Fu et al., which showed the catalytic activity in aqueous hydrogenations five times higher than that of the commercial Pd/C catalyst [20].

Polyacrylonitrile fiber (PANF) is one of the support materials in which the surface microenvironment can be tuned to make the catalytic sites highly efficient. PANF, widely used in textile industry, has advantages such as low cost, easy availability, high mechanical strength, corrosion resistance and braid-ability [23, 24]. It contains sufficient cyano groups that can form carboxyl, amido or other groups through facile reactions [25, 26]. In our previous reports, PANF has been used to immobilize quaternary ammonium salt [25], phosphorous acid [27], pyrrolidine [28], tertiary amine [29], L-lysine [30], etc., making functionalized fiber catalysts with high activity, simple preparation and good recyclability [31, 32]. The immobilization process generates middle and deep modification in the surface, so that a special microenvironment surrounding active site is constructed, which helps to improve the catalytic performance [26, 33].

However, in the abovementioned reports, the microenvironments of heterogeneous catalysts have been tuned by introducing interchain auxiliary groups near the catalytic sites [19, 34]. In this work, a novel microenvironment regulation method was designed to synthesize a fiber catalyst with intrachain quaternary ammonium salt (QA) moiety in the inner side of the catalytically active tertiary amine (TA) sites; thus a series of catalysts ($PAN_{PQ\text{-}n}F$, n = 0.1–1) with QA and TA bifunctionalized structure were prepared (Scheme 1), in which a special microenvironment of hydrophobic inner and hydrophilic outer layer were successfully constructed.

Aza-Michael addition of nitrogen nucleophiles to electron-deficient alkenes is a common method for C-N bond formation and has important applications in the synthesis of *N*-containing compounds, such as *β*-aminocarbonyls and *N*-containing heterocycles in many antibiotics and pharmaceutical intermediates [35, 36]. Aza-Michael addition can be catalyzed by organic amine [37] or ionic liquids [38–40], which indicates that the $PAN_{PQ\text{-}n}F$ with both QA and TA moieties has the potential to catalyze this reaction. Therefore, different microenvironments in the fiber surface were investigated by using aza-Michael addition of chalcone and aniline as a probe, and the effect of the ratio of QA to TA on the catalytic activity and recyclability was elucidated.

2 Experimental

2.1 Synthesis of the Fiber Catalysts

The QA and TA bifunctionalized polyacrylonitrile fibers $PAN_{PQ\text{-}n}Fs$ were synthesized via two steps (Scheme 1).

Step 1: The mixture of PANF (1 g), *N*-(2-aminoethyl) piperazine (15 mL) and deionized water (15 mL) was refluxed for 8 h. Then the fiber was taken out and washed with hot water (60–70 °C) until neutral. The fiber was dried overnight at 60 °C under vacuum to gain PAN_PF. The weight gain of PAN_PF based on PANF was 27% with the functionality of 1.6 mmol/g.

Step 2: The mixture of PAN_PF (0.5 g), benzyl bromide (5 g), acetonitrile (15 mL) and Na_2CO_3 (0.045 g) was refluxed for 0.5–8 h to get different proportions of QA and TA (Table 1). Afterwards, the fiber was taken out and washed with hot water (60–70 °C). Then the fiber was stirred in saturated Na_2CO_3 solution overnight and washed with hot water (60–70 °C) until neutral. The excess benzyl bromide on the fiber was extracted using Soxhlet extraction apparatus and ethanol as solvent for more than 6 h. The fiber was dried overnight at 60 °C under vacuum to gain $PAN_{PQ\text{-}n}Fs$ (n = 0.1–1).

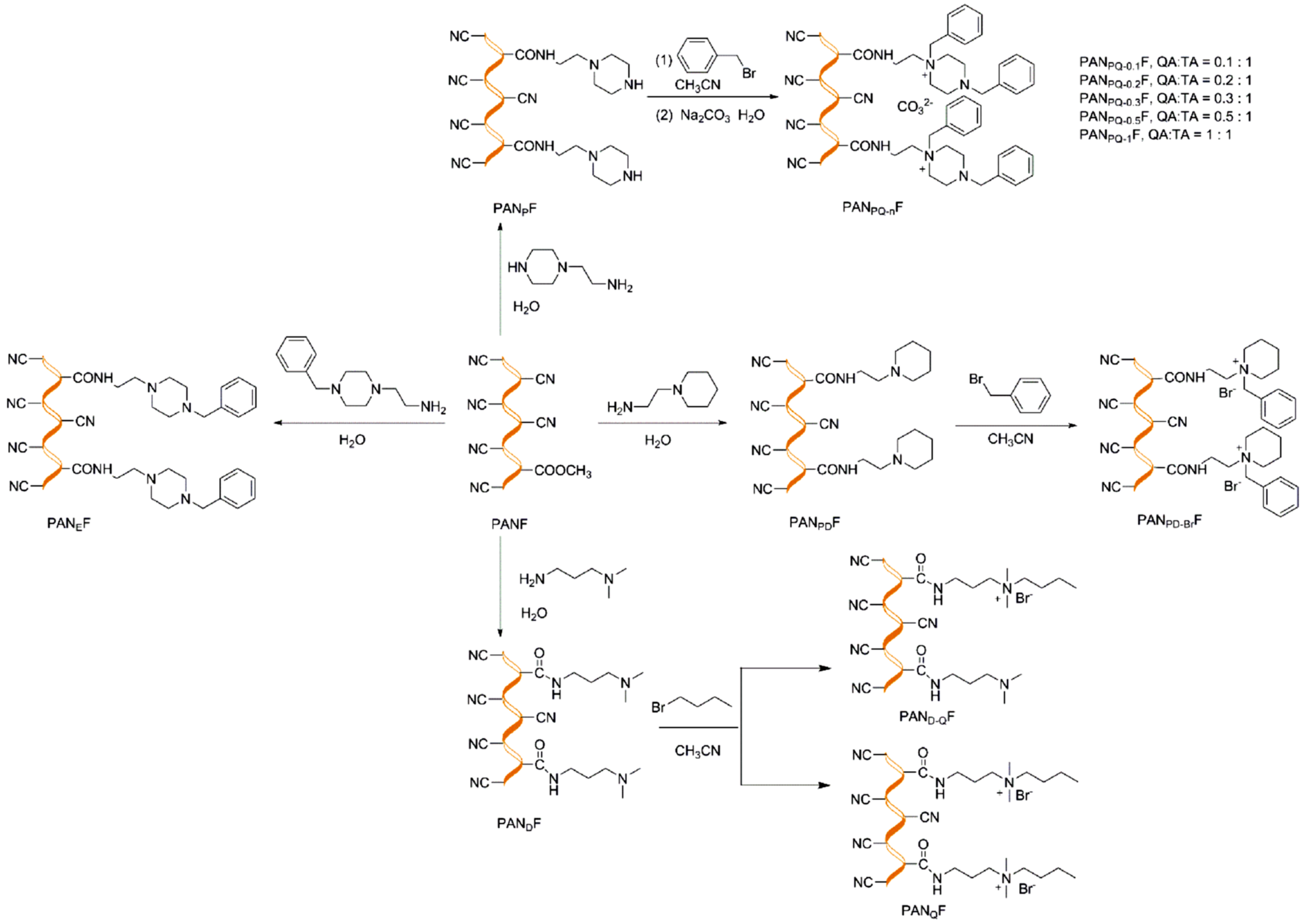

Scheme 1 The general synthetic steps of fiber catalysts

Table 1 Adjust the ratio of QA to tertiary TA of $PAN_{PQ\text{-}n}Fs$

Entry	Benzyl bromide (g)	Solvent (15 mL)	Temperature (°C)	Time (h)	QA:TA
1	5	CH_3CN	80	0.5	0.1:1
2	5	CH_3CN	80	3	0.2:1
3	5	CH_3CN	80	4	0.3:1
4	5	CH_3CN	80	5	0.5:1
5	5	CH_3CN	80	8	1:1

PAN_PF (weight gain 27%, functional degree 1.6 mmol/g, 1 g)

Add Na_2CO_3 (0.17 g) into mixture

2.2 Characterization of the Fiber Catalysts

The Fourier transform infrared (FT-IR) spectra were obtained using an AVATAR360 FTIR spectrometer (Thermo Nicolet). The elemental analysis (EA) was performed on a vario micro cube (Elementar). The X-ray powder diffraction patterns (XRD) were obtained using a D/MAX-2500 X-ray diffractometer (Rigaku Corporation). The thermogravimetric analysis (TGA) of fiber samples were measured by STA409PC TGA/DSC (Netzsch company, Germany). The mechanical properties of different fiber catalyst samples were tested with an electronic single fiber strength tester YG(B)001A (Wenzhou Darong Textile Instrument Corporation, China). The X-ray photoelectron spectra (XPS) were performed on PH1600 spectrometer (PERKIN ELMZR). The water contact angles of fibers were determined using OCA15EC (DataPhysics company, Germany). The fibers surface morphology was characterized by scanning electron microscope (SEM) (Hitachi, model S-4800). The analyses of HPLC were performed on Waters Model 510. The ^1H NMR spectra were obtained by BRUKER-AVANCE III (400 MHz) instruments using TMS (tetramethylsilane) as the internal standard.

2.3 General Procedure for Aza-Michael Addition

The mixture of chalcone (0.5 mmol), aniline (1 mmol), fiber catalyst (10 mol%) and water (3 mL) were stirred at 60 °C for 10 h. After completion of the reaction, the mixture was cooled to room temperature. The fiber catalyst was taken out with tweezers and washed with methylene chloride (5 mL × 3) and ethanol (5 mL × 3). The filtrate was combined with the remaining reaction mixture and a small aliquot was taken out for HPLC analysis with the nitrobenzene as internal standard.

3 Results and Discussion

3.1 Preparation of $PAN_{PQ\text{-}n}Fs$

The QA and TA bifunctionalized polyacrylonitrile fibers ($PAN_{PQ\text{-}n}Fs$) were synthesized by two simple steps (Scheme 1). The functionality of $PAN_{PQ\text{-}n}Fs$ were determined by weight gain. The formula for weight gain is: $weightgain = \left[(w2 - w1)/w1\right] \times 100\%$, in which w_1 and w_2 are the weights of the original and functionalized fiber, respectively.

The weight gain of $PAN_{PQ\text{-}n}Fs$ can be easily adjusted by changing the preparation conditions, including the functionalization degree of PAN_PF, benzyl bromide concentration, reaction temperature and time. After further balancing of functionalization and mechanical strength, the weight gain of PAN_PF about 27% was preferred. The ratio of quaternary ammonium (QA) to tertiary amine (TA) in the target fiber $PAN_{PQ\text{-}n}Fs$ were adjusted by varying the reaction time of the selected PAN_PF fiber (Table 1). With grafting time more than 8 h, the proportion of QA could not be increased further. To avoid the decrease of mechanical strength, the grafting time was no longer prolonged.

3.2 Characterization of the Fiber

3.2.1 Fourier Transform Infrared Spectroscopy (FT-IR)

Before FT-IR measurement, the fiber sample was shredded and made into pellets with KBr. As shown in Fig. 1, the FT-IR spectrum of PANF (Fig. 1a) has two characteristic absorption peaks at 2244 cm^{-1} and 1734 cm^{-1} which attribute to the C≡N and C=O stretching vibrations, respectively. Compared with PANF, the functionalized fibers have a broad absorption peak around 3500 cm^{-1} caused by the stretching vibration of N–H, which proves the successful aminolysis of –C≡N associated with the weakening of the peak at 2244 cm^{-1}. The peak at 1651 cm^{-1} is attributed to the stretching vibration of C=O in amide.

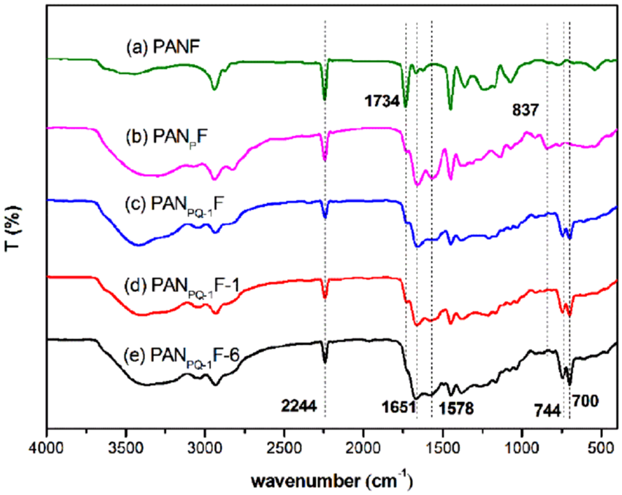

Fig. 1 FT-IR spectra of (a) PANF, (b) PAN_PF, (c) $PAN_{PQ\text{-}1}F$, (d) $PAN_{PQ\text{-}1}F\text{-}1$, and (e) $PAN_{PQ\text{-}1}F\text{-}6$

In the spectrum of PAN_PF (Fig. 1b), the appearance of a peak at 1578 cm^{-1} is due to the bending vibration of N–H in CONH, and the obvious peak at 837 cm^{-1} is attributed to the bending vibration of the N–H in the secondary amine. Both of them indicate the successful grafting of *N*-aminoethylpiperazine on PANF. Furthermore, in the spectrum of $PAN_{PQ\text{-}1}F$ (Fig. 1c), the appearance of the peaks at 744 cm^{-1} and 700 cm^{-1} can support the successful grafting of benzyl groups in the PAN_PF; the decrease of the peak at 837 cm^{-1} can also ndicate the consumption of secondary amine. What's more, the FT-IR spectra of $PAN_{PQ\text{-}1}F\text{-}1$ and $PAN_{PQ\text{-}1}F\text{-}6$ show that the absorption peaks of the catalyst $PAN_{PQ\text{-}1}F$ remained unchanged after being used once and six times, indicating that the fiber catalyst was stable enough for multiple use.

3.2.2 Elemental Analysis (EA)

As shown in Table S5, because of the lower carbon content and higher hydrogen content of *N*-(2-aminoethyl) piperazine, the carbon content of the PAN_PF decreased expectedly and the hydrogen content increased compared with original fiber PANF (Table S5, Entry 2). After further treatment of PAN_PF with benzyl bromide, the hydrogen and nitrogen contents of $PAN_{PQ\text{-}1}F$ decreased and the carbon content increased in accordance with the carbon, nitrogen and hydrogen contents of benzyl group (Table S5, Entry 3). After the $PAN_{PQ\text{-}1}F$ was used six times, there was a slight change in the EA data of the $PAN_{PQ\text{-}1}F\text{-}6$ (Table S5, Entry 5). This change may be caused by the slight adsorption of the reactants or product on the surface of the fiber catalyst.

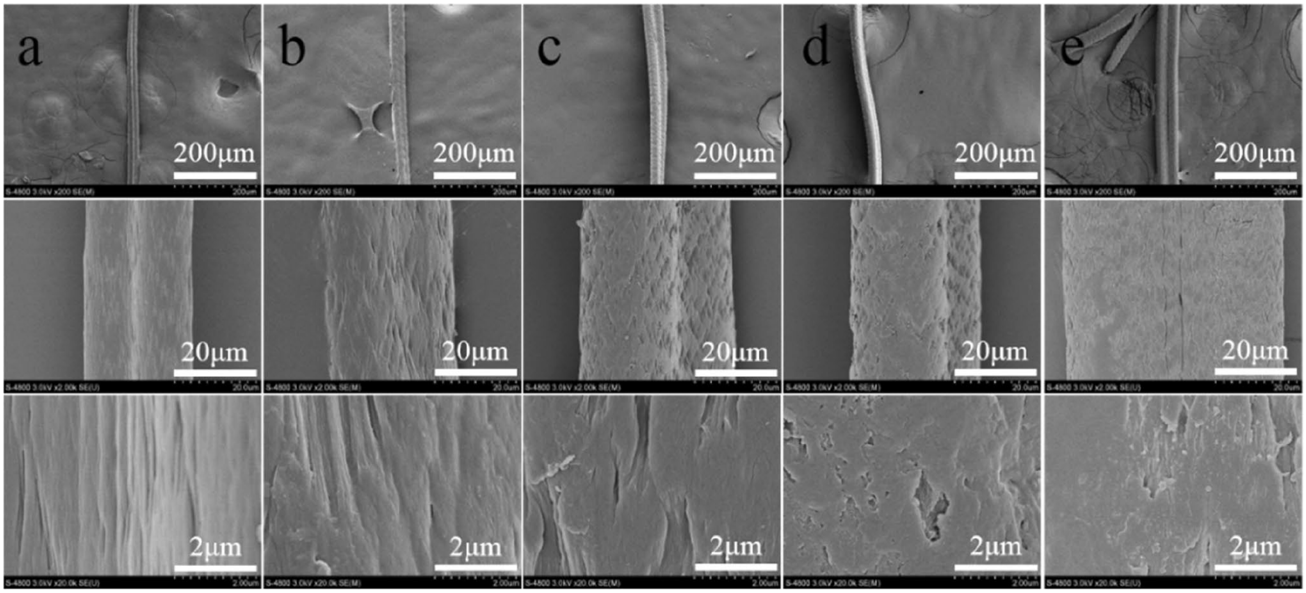

Fig. 2 SEM images of **a** PANF, **b** PAN$_P$F, **c** PAN$_{PQ\text{-}1}$F, **d** PAN$_{PQ\text{-}1}$F-1, and **e** PAN$_{PQ\text{-}1}$F-6

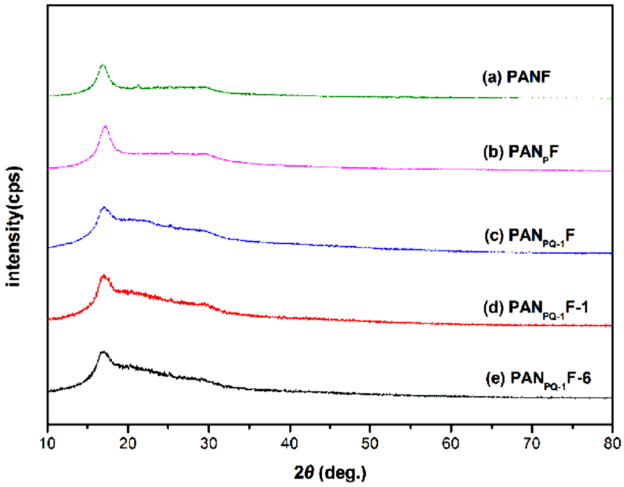

Fig. 3 X-ray diffraction spectra of (a) PANF, (b) PAN$_P$F, (c) PAN$_{PQ\text{-}1}$F, (d) PAN$_{PQ\text{-}1}$F-1, and (e) PAN$_{PQ\text{-}1}$F-6

3.2.3 Scanning Electron Microscope (SEM)

The SEM images of PANF, PAN$_P$F, PAN$_{PQ\text{-}1}$F, PAN$_{PQ\text{-}1}$F-1 and PAN$_{PQ\text{-}1}$F-6 are shown in Fig. 2. It can be seen from the Fig. 2 that PAN$_P$F and PAN$_{PQ\text{-}1}$F become thicker compared with PANF, which can prove the successful grafting of small molecules (Fig. 2a, b, c). In addition, after the fiber was used 6 runs, the surface of PAN$_{PB\text{-}5}$F-6 was rougher and had more cracks, but there was no serious damage which indicated that the fiber had good physical tolerance during recycling (Fig. 2e).

Table 2 Mechanical properties of different fibers

Entry	Fiber	BS (cN)	RBS (%)
1	PANF	10.67	100
2	PAN$_P$F	10.17	95
3	PAN$_{PQ\text{-}1}$F	9.57	90
4	PAN$_{PQ\text{-}1}$F-1	8.57	80
5	PAN$_{PQ\text{-}1}$F-6	7.86	74

3.2.4 X-ray Diffraction (XRD)

The XRD pattern of PANF (Fig. 3a) shows a main diffraction peak at 17° and a weak peak centered at 29.5°, corresponding to the (100) and (110) crystallographic planes of the PANF hexagonal lattice, respectively [27, 32, 41]. After modification, the patterns of PAN$_P$F and PAN$_{PQ\text{-}1}$F remained similar to that of PANF, which indicates that the grafting of small molecules doesn't change the crystal structure of PANF. Even after being used six times, the diffractogram of PAN$_{PQ\text{-}1}$F-6 remained unchanged, proving that the crystal structure of PAN$_{PQ\text{-}1}$F wasn't damaged after reuse.

3.2.5 Breaking Strength (BS)

The BS and retention of breaking strength (RBS) of fibers are shown in Table 2. Compared with the original fiber, the breaking strength of PAN$_{PQ\text{-}1}$F decreased from 10.67 to 9.57 with 90% RBS (Table 2, Entry 3). After being used six times, due to the long-time mechanical stirring and heating, the PAN$_{PQ\text{-}1}$F-6 breaking strength was decreased from 9.57

to 7.86, but still maintained 82% breaking strength compared with the $\mathrm{PAN_{PQ\text{-}1}F}$ (Table 2, Entry 5), indicating that the functionalized fibers have good mechanical strength for reuse.

3.2.6 Thermogravimetric Analysis (TGA)

Thermogravimetric analysis is used to evaluate the thermal stability of the functionalized fibers. The samples were heated in nitrogen gradually from room temperature to 800 °C. As shown in Fig. S1, from room temperature to 300 °C, PANF had almost no weight loss, indicating that the fiber support has high thermal stability. The $\mathrm{PAN_PF}$ and $\mathrm{PAN_{PQ\text{-}1}F}$ had slight mass loss ($<6\%$) below 200 °C due to possible dehydration, which implies that the functional fibers have good thermal stability and can be applied in a wide temperature range. Compared with $\mathrm{PAN_{PQ\text{-}1}F}$, $\mathrm{PAN_PF}$ had more mass loss at 200 °C, mainly because it absorbed more water via stronger hydrogen bonding between amine N–H and water molecule. The functional fibers were decomposed when the temperature was higher than 200 °C. It was probably caused by decomposition of QA and TA moieties and structural damage of fiber matrix.

3.2.7 X-Ray Photoelectron Spectroscopy (XPS)

The fiber surface composition can be characterized by XPS. The XPS spectra of PANF, $\mathrm{PAN_PF}$, $\mathrm{PAN_{PQ\text{-}1}F}$ and $\mathrm{PAN_{PQ\text{-}Br}F}$ (Scheme S1) are presented in Fig. 4. The high resolution C 1s spectrum for the $\mathrm{PAN_{PQ\text{-}1}F}$ can be deconvoluted into three species, near 284.7, 286.5, and 288.3 eV, which are attributed to carbon from C–N/C–O, C≡N, and N–C=O, respectively (Fig. S2) [27, 32, 42, 43]. The high resolution N 1s spectrum for the $\mathrm{PAN_{PQ\text{-}1}F}$ has two peaks at 399.6 and 402.1 eV, corresponding to N–C=O/N(C)$_3$ and N$^+$ respectively (Fig. S2) [43]. To sum up, the XPS spectrum of $\mathrm{PAN_{PQ\text{-}1}F}$ further demonstrates the successful grafting of the fibers.

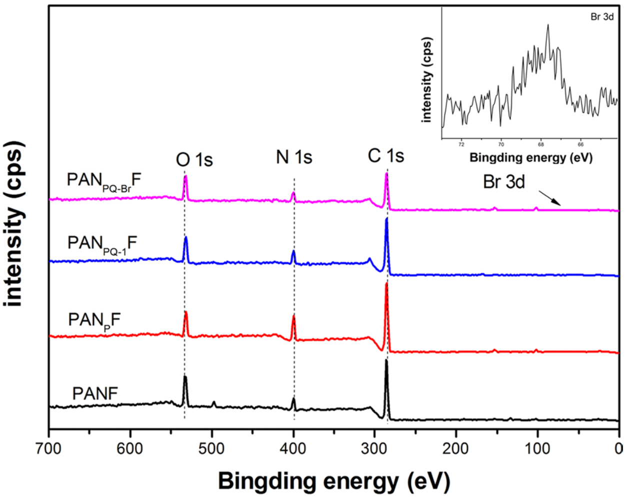

Fig. 4 XPS spectra of PANF, $\mathrm{PAN_PF}$, $\mathrm{PAN_{PQ\text{-}1}F}$ and $\mathrm{PAN_{PQ\text{-}Br}F}$

3.3 Catalytic Properties of Bifunctionalized Fiber Catalysts in Aza-Michael Addition

To investigate the microenvironments of fiber catalysts, the reaction of aniline with chalcone in water was used as a model reaction. Without any catalyst or in the presence of PANF and $\mathrm{PAN_PF}$, the yields of the reaction were very low, which indicated that neither cyano groups in PANF nor amido and amino groups in $\mathrm{PAN_PF}$ could catalyze the reaction (Table 3, Entry 1–3). However, the yield by $\mathrm{PAN_{PQ\text{-}0.1}F}$ catalysis was significantly improved (Table 3, Entry 4). The ratio of QA to TA changed gradually by prolonging the grafting time of $\mathrm{PAN_PF}$ (Table 1). The results showed that the catalytic performance increased gradually as the content of QA moiety increased (Table 3, Entry 4–8). When the ratio of QA to TA equals 1: 1, the catalytic performance was the best (Table 3, Entry 8). Using the fiber catalyst $\mathrm{PAN_EF}$ with only TA groups, the catalytic activity decreased obviously and the yield was only 32% (Scheme 1; Table 3, Entry 9). Using the fiber $\mathrm{PAN_{PD\text{-}Br}F}$ with only QA groups as a catalyst, the yield decreased to 19% (Scheme 1; Table 3, Entry 10). Therefore, QA and TA showed cooperative effect in $\mathrm{PAN_{PQ\text{-}1}F}$-catalyzed aza-Michael addition.

The cooperative catalysis can also be demonstrated by the $\mathrm{PAN_{D\text{-}Q}F}$ (Scheme 1). The yield was 88% in the presence of $\mathrm{PAN_DF}$ (Table 3, Entry 11). The $\mathrm{PAN_DF}$ was further reacted with benzyl bromide to obtain $\mathrm{PAN_{D\text{-}Q}F}$, which had both QA and TA moieties. The $\mathrm{PAN_{D\text{-}Q}F}$ catalytic yield was up to 98%, indicating that both QA and TA were involved in the cooperative catalysis (Table 3, Entry 13). After converting all the TA groups of the $\mathrm{PAN_DF}$ into QA to obtain the $\mathrm{PAN_QF}$, the yield decreased to 19%, indicating that the catalytic activity was poor when only QA groups was present (Table 3, Entry 12). However, the product was densely adsorbed onto $\mathrm{PAN_{D\text{-}Q}F}$ surface and was difficult to separate after the reaction was completed, which didn't happen in $\mathrm{PAN_{PQ\text{-}1}F}$ catalysis.

The different catalytic phenomena and activities between $\mathrm{PAN_{PQ\text{-}1}F}$ and $\mathrm{PAN_{D\text{-}Q}F}$ can be attributed to the different fiber microenvironments (Fig. 5). In the microenvironment constructed with separated interchain QA and TA moieties into $\mathrm{PAN_{D\text{-}Q}F}$ surface, hydrophobic product molecules accumulated around hydrophobic active sites of TA, which inhibited the recovery of active sites for catalytic cycle. However, by decorating QA and TA in the same molecular chain, the $\mathrm{PAN_{PQ\text{-}1}F}$ had a special microenvironment with hydrophobic outer layer and hydrophilic inner layer, which was beneficial to the swelling of the

Table 3 Catalytic activities of different fiber catalysts

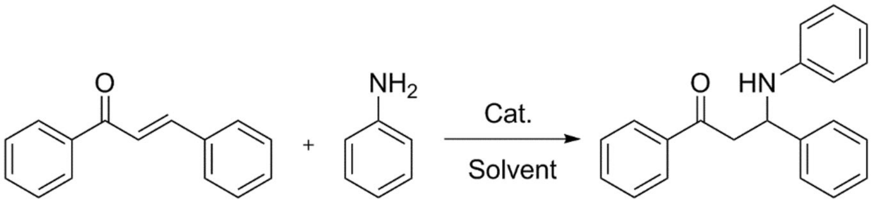

Entry	Catalyst	Dosage	Temperature (°C)	Solvent	Time (h)	Yield (%)[a]
1	Blank	–	50	H_2O	12	2
2	PANF	20 mol%	50	H_2O	12	3
3	PAN_PF	20 mol%	50	H_2O	12	9
4	$PAN_{PQ\text{-}0.1}F$	20 mol%	50	H_2O	12	57
5	$PAN_{PQ\text{-}0.2}F$	20 mol%	50	H_2O	12	84
6	$PAN_{PQ\text{-}0.3}F$	20 mol%	50	H_2O	12	89
7	$PAN_{PQ\text{-}0.5}F$	20 mol%	50	H_2O	12	93
8	$PAN_{PQ\text{-}1}F$	20 mol%	50	H_2O	12	99
9	PAN_EF	20 mol%	50	H_2O	12	32
10	$PAN_{PD\text{-}Br}F$	20 mol%	50	H_2O	12	17
11	PAN_DF	20 mol%	50	H_2O	24	88
12	PAN_QF	20 mol%	50	H_2O	24	19
13	$PAN_{D\text{-}Q}F$	20 mol%	50	H_2O	24	98

Reaction conditions: chalcone (0.5 mmol), aniline (1 mmol) in 3 mL of solvent and the fiber catalyst dosage was based on TA (1.3 mmol/g)

[a] Measured by HPLC with nitrobenzene as the internal standard

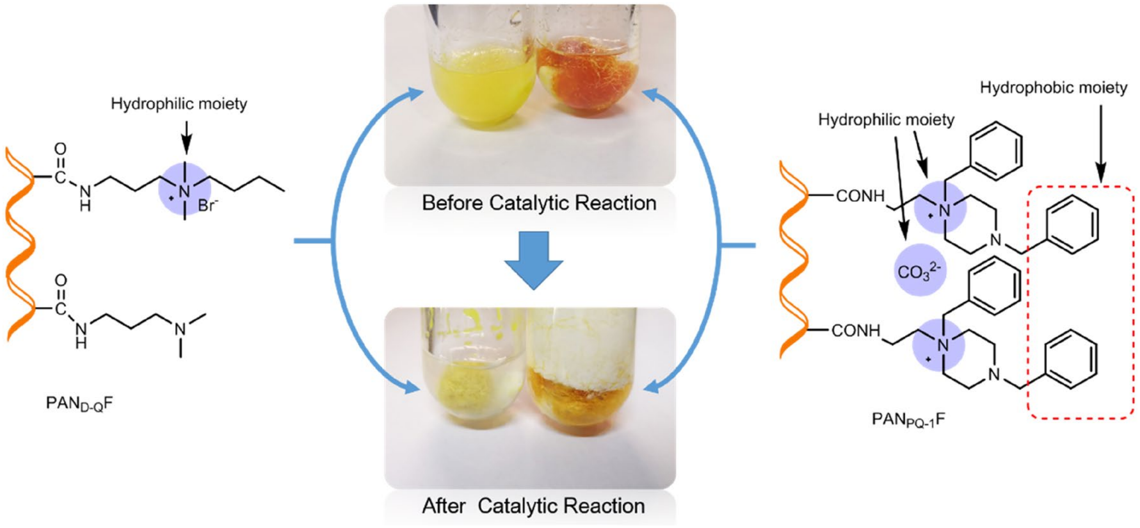

Fig. 5 The microenvironment of $PAN_{PQ\text{-}1}F$ and $PAN_{D\text{-}Q}F$

fiber in water. The reactants were easily enriched in outer layer during stirring, and they interacted with the catalytic TA sites to yield the addition product. Afterward, the hydrophilic inner layer of $PAN_{PQ\text{-}1}F$ had a certain repulsion to hydrophobic product molecule, which facilitated its movement out of the microenvironment, and made the active TA sites free and highly exposed to next catalytic cycle. As such, tuning of microenvironment near the active sites affected their catalytic efficiency via different desorption (Fig. 6).

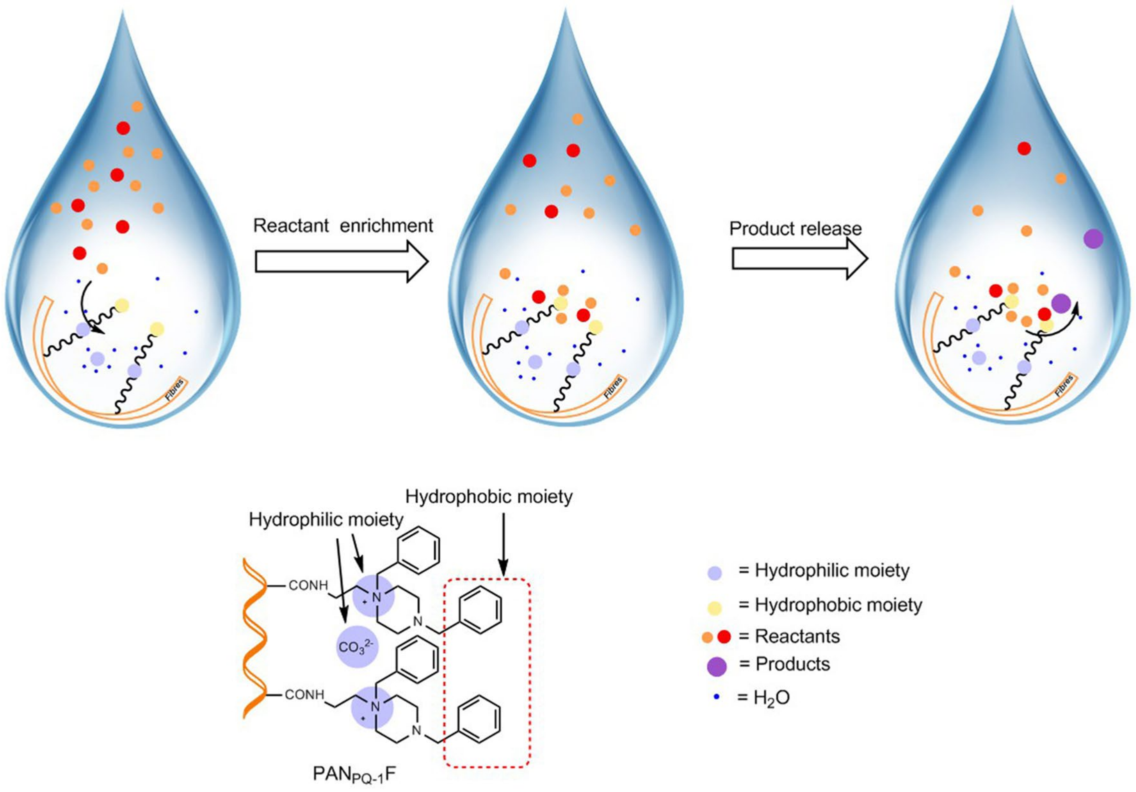

Fig. 6 Possible microenvironment of fiber for the aza-Michael addition catalyzed by $PAN_{PQ-1}F$

After that, the effect of different anions of the fiber catalyst on the activity was investigated. As shown in Scheme S4, five fiber catalysts with different anions had been prepared. The experimental results showed that changing the anion of the fiber catalysts had a great effect on their performance. When the anion was CO_3^{2-}, its catalytic activity was the highest (Table S3, Entry 1–6).

Moreover, the reaction conditions of catalytic aza-Michael addition were optimized (Table 4), and different solvents were screened (Table 4, Entry 1–10). Because of special microenvironment in the fiber surface, the $PAN_{PQ-1}F$ had good solvent selectivity, and the reaction had high yields only in water (Table 4, Entry 1). The optimal conditions for the reaction were 10 mol% $PAN_{PQ-1}F$, 60 °C, 10 h, and water as the solvent (Table 4, Entry 20).

3.4 Aza-Michael Addition of Different Amines and Chalcone

To investigate the reaction scope, aza-Michael addition of different amines and chalcone was explored under the optimal reaction conditions. As shown in Table 5, most products were obtained with excellent yields. The electron-donating groups on benzene ring of aniline such as $–CH_3$ and $–OCH_3$ were favorable, and more than 93% yields could be obtained in short time. However, there was no target product when the substituent $–CH_3$ was in the ortho position, indicating that the reaction is greatly affected by the steric hindrance. When the substituents were electron-withdrawing groups, different phenomena were observed. When the substituent was –Cl at the para position, the yield could reach more than 94% in a short time, and the good yield could be obtained by prolonging the reaction time with meta-Cl, indicating that the position of the substituent had a significant effect on the reaction. When the substituent was $–COOCH_3$, the reaction was conducted at 60 °C for above 36 h to get an 80% yield. By increasing the reaction temperature to 80 °C, a yield of 97% could be achieved in 10 h. However, when the substituent was $–NO_2$, the target product couldn't be obtained when the temperature was increased or the reaction time was prolonged. It was probably because the strong electron uptake of $–NO_2$ led to the decrease of amino activity. In summary, the $PAN_{PQ-1}F$ can effectively catalyze aza-Michael addition with wide substrate scope and no by-products were observed.

3.5 Possible Mechanism of $PAN_{PQ-1}F$-Catalyzed Aza-Michael Addition

A possible mechanism of aza-Michael addition of chalcone with aniline catalyzed by $PAN_{PQ-1}F$ was described

Table 4 Optimization of the aza-Michael addition

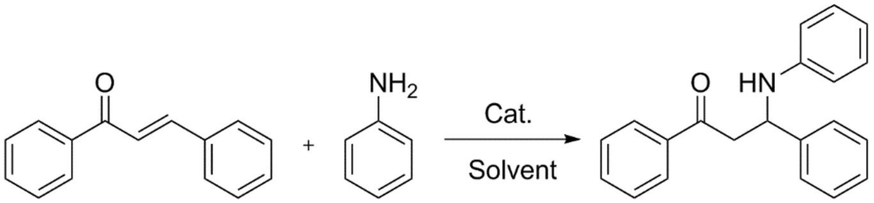

Entry	Catalyst	Dosage[a]	Temperature (°C)	Solvent	Time (h)	Yield (%)[b]
1	$PAN_{PQ\text{-}1}F$	10 mol%	50	H_2O	10	91
2	$PAN_{PQ\text{-}1}F$	10 mol%	50	EtOH	10	12
3	$PAN_{PQ\text{-}1}F$	10 mol%	50	CH_3OH	10	16
4	$PAN_{PQ\text{-}1}F$	10 mol%	50	CH_3CN	10	3
5	$PAN_{PQ\text{-}1}F$	10 mol%	50	EtOAc	10	1
6	$PAN_{PQ\text{-}1}F$	10 mol%	50	DMF	10	4
7	$PAN_{PQ\text{-}1}F$	10 mol%	50	THF	10	1
8	$PAN_{PQ\text{-}1}F$	10 mol%	50	1,4-Dioxane	10	1
9	$PAN_{PQ\text{-}1}F$	10 mol%	50	Cyclohexane	10	2
10	$PAN_{PQ\text{-}1}F$	10 mol%	50	Toluene	10	28
11	$PAN_{PQ\text{-}1}F$	10 mol%	25	H_2O	6	33
12	$PAN_{PQ\text{-}1}F$	10 mol%	50	H_2O	6	77
13	$PAN_{PQ\text{-}1}F$	10 mol%	60	H_2O	6	84
14	$PAN_{PQ\text{-}1}F$	10 mol%	70	H_2O	6	86
15	$PAN_{PQ\text{-}1}F$	10 mol%	80	H_2O	6	85
16	$PAN_{PQ\text{-}1}F$	10 mol%	100	H_2O	6	49
17	$PAN_{PQ\text{-}1}F$	20 mol%	60	H_2O	12	99
18	$PAN_{PQ\text{-}1}F$	10 mol%	60	H_2O	12	99
19	$PAN_{PQ\text{-}1}F$	5 mol%	60	H_2O	12	77
20	$PAN_{PQ\text{-}1}F$	10 mol%	60	H_2O	10	99
21	$PAN_{PQ\text{-}1}F$	10 mol%	60	H_2O	8	89

Reaction conditions: chalcone (0.5 mmol), aniline (1 mmol), H_2O (3 mL)

[a] Based on TA

[b] Measured by HPLC with nitrobenzene as the internal standard

in Scheme 2, indicating the cooperative catalysis of QA and TA. Initially, the TA in $PAN_{PQ\text{-}1}F$ acted as a nucleophile, in which N atom attacked electron-deficient alkene to form an active intermediate A. Then the CO_3^{2-} moved outward to activate aniline through hydrogen bonding [44–46], which improved the nucleophilicity of aniline, then promoted the key nucleophilic substitution of intermediate A and the proton transfer from aniline to CO_3^{2-}. Subsequently, TA on the fiber catalyst was released to form the enolate intermediate in B, which accepted proton from HCO_3^- and underwent keto-enol tautomerization to form the addition product. Eventually, the product molecule was expelled out of the microenvironment by hydrophilic inner layer, especially with the aid of CO_3^{2-}. The surface microenvironment of $PAN_{PQ\text{-}1}F$ was recovered and the catalytic sites were highly exposed for the next catalytic cycle (Fig. 6). Therefore, QA in $PAN_{PQ\text{-}1}F$ has two functions: N cation constructs the inner hydrophilic layer associated with CO_3^{2-} to facilitate the desorption of product molecule and enhance the catalytic efficiency of active TA sites; carbonate ion activates aniline nucleophile and also mediates proton transfer. To the best of our knowledge, this type of tuning method of microenvironment around active sites and the resulting cooperative catalysis mode of QA with TA have not been reported, although there have been scarce reports on cooperative heterogeneous catalysis by QA and TA, for example, Yin et al. reported that the cooperative effect of QA and TA in GO-immobilized urotropin derivative for catalytic CO_2 cycloaddition [47].

Table 5 $PAN_{PQ\text{-}1}F$ catalyzed aza-Michael addition of various amines and chalcone

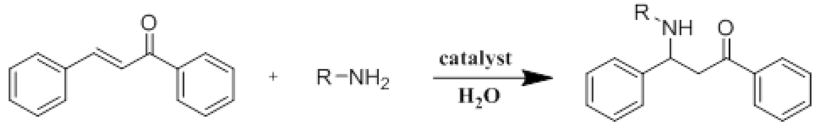

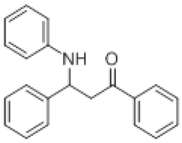	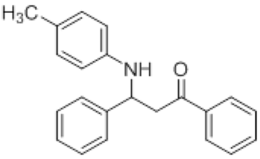	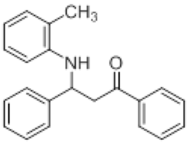	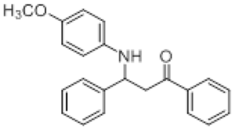
5a 99% 60 °C 10 h	**5b 93% 60 °C 9 h**	**5c None 80 °C 48 h**	**5d 94% 60 °C 10 h**
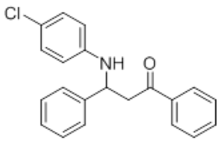	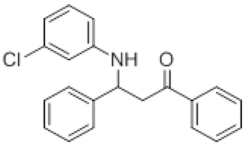	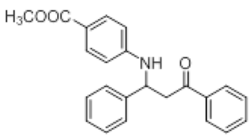	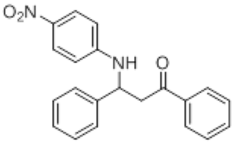
5e 94% 60 °C 10 h	**5f 94% 60 °C 16 h**	**5g 97% 80 °C 10 h**	**5h None 80 °C 48 h**

Reaction conditions: chalcone (1 mmol), aniline (2 mmol), and catalyst dosage of 10 mol% based on tertiary amine content ($PAN_{PQ\text{-}1}F$)

Isolated yield

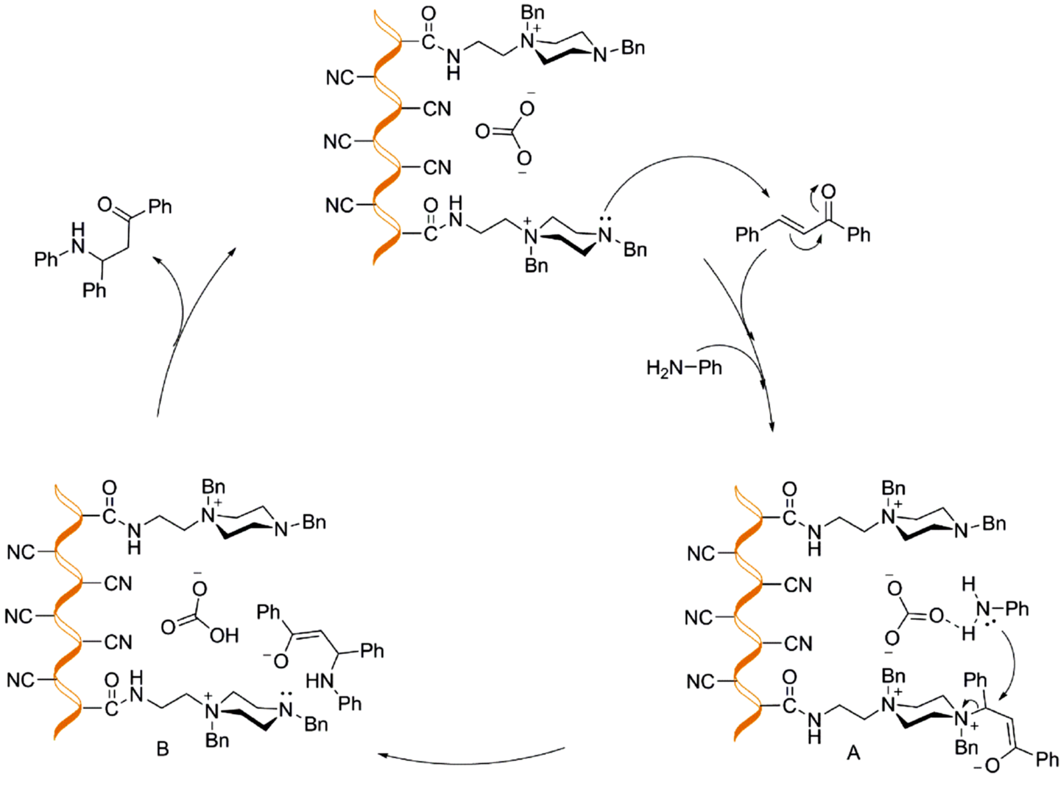

Scheme 2 Possible mechanism of the aza-Michael addition catalyzed by $PAN_{PQ\text{-}1}F$

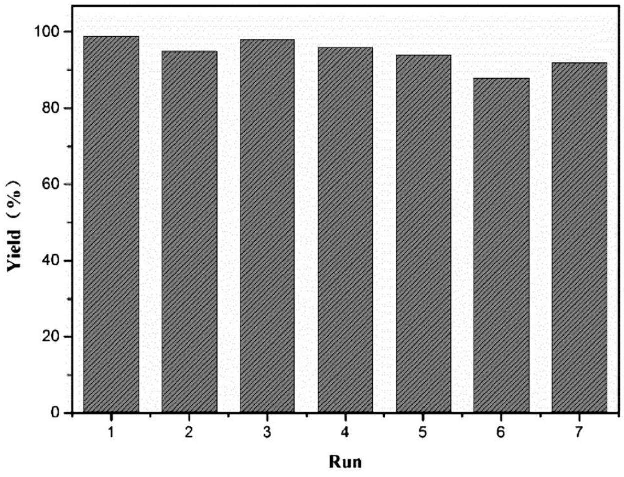

Fig. 7 Recyclability of $\mathrm{PAN_{PQ\text{-}1}F}$ in aza-Michael addition

3.6 Recyclability and Stability of the Catalyst $\mathrm{PAN_{PQ\text{-}1}F}$

The recyclability of the $\mathrm{PAN_{PQ\text{-}1}F}$ catalyst in the aza-Michael addition of chalcone (0.5 mmol) and aniline (1 mmol) in water (3 mL) was investigated at 60 °C for 10 h (Fig. 7). The results showed that the reaction proceeded smoothly with the recycled catalyst, and the yield almost did not decrease after 6 runs. The used $\mathrm{PAN_{PQ\text{-}1}F}$ was simply taken out with tweezers, washed with methylene chloride, ethanol and water, and put into the next run without further treatment. When the $\mathrm{PAN_{PQ\text{-}1}F}$ catalyst was used for the sixth run, the yield decreased to 88%. In the seventh run, the yield could be increased to 92% with the extension of reaction time to 12 h. Probably because the mechanical strength of $\mathrm{PAN_{PQ\text{-}1}F}$ was decreased and the adsorption of product into the surface of $\mathrm{PAN_{PQ\text{-}1}F}$, the catalytic activity of the fiber decreased after being used 6 times.

4 Conclusion

In summary, a novel type of quaternary ammonium salt and tertiary amine intrachain bifunctionalized polyacrylonitrile fibers were successfully prepared to catalyze the aza-Michael addition in water. When the ratio of two functional groups was 1:1 ($\mathrm{PAN_{PQ\text{-}1}F}$), the highest catalytic performance was achieved under mild conditions, and both the quaternary ammonium salt and the tertiary amine of the catalyst $\mathrm{PAN_{PQ\text{-}1}F}$ had the highest cooperative catalysis effect. Moreover, without significant fiber structural damage, $\mathrm{PAN_{PQ\text{-}1}F}$ can be reused more than 6 times under optimal conditions with highly catalytic activity. This fiber catalyst has the advantages of simple preparation, strong durability, high activity, adjustable microenvironment, easy recovery, low cost and environmental friendliness, showing great practical potential in chemical industry. The unique microenvironment with outer hydrophobicity and inner hydrophilicity was proposed to explain the different desorption of the formed product, and novel cooperative catalysis mode of tertiary amino, quaternary ammonium and carbonate ion was elucidated.

Acknowledgements This work was financially supported by the National Natural Science Foundation of China (No. 21777111).

References

1. Ferré M, Pleixats R, Wong Chi Man M (2016) Green Chem 18:881
2. Siddiqui S, Khan MU, Siddiqui ZN (2017) ACS Sustain Chem Eng 5:7932
3. Dijkmans J, Gabriëls D, Dusselier M (2013) Green Chem 15:2777
4. SánchezVelandia JE, Gelves JF, Márquez MA (2020) Catal Lett. https://doi.org/10.1007/s10562-020-03225-9
5. Liang J, Yu Q, Yang X (2018) Nano Res 11:1599
6. Jin Z, Xiao M, Bao Z (2012) Angew Chem Int Ed 51:6406
7. Reddy SS, Kalla RMN, Varyambath A (2019) Catal Commun 126:15
8. Lee JW, Thomas MG, Opwis K (2013) Science 341:1225
9. Wen J, Chen Y, Ji S (2019) Nano Res 12:2584
10. Deng Q, Wen X, Zhang P (2019) Catal Commun 126:5
11. Ding QD, Si JP, Huang KL (2019) Catal Commun 127:69
12. Feng J, He Y, Liu Y (2015) Chem Soc Rev 44:5291
13. Azizi N, Saidi MR (2005) Org Lett 7:3649
14. Ravenelle RM, Schüβler F, D'Amico A (2010) J Phys Chem C 114:19582
15. Zhang L, Chen K, Chen B (2015) J Am Chem Soc 137:11810
16. Gibson LT (2014) Chem Soc Rev 43:5173
17. Bass JD, Solovyov A, Pascall AJ (2006) J Am Chem Soc 128:3737
18. Wang C, Leng S, Guo H (2019) Appl Surf Sci 478:319
19. Bonomi P, Bavaro T, Serra I (2013) Molecules 18:14349
20. Fu L, Li S, Han Z (2014) Chem Commun 50:10045
21. Xue F, Zhang Y, Zhang F (2017) ACS Appl Mater Interfaces 9:8403
22. Zhao L, Shi S, Liu M (2019) ChemCatChem 12:903
23. Xiao J, Xu G, Wang L (2019) J Ind Eng Chem 77:65
24. Wang B, Chen PY, Zhao RX (2019) Chem Eng J. https://doi.org/10.1016/j.cej.2019.123484
25. Du J, Xu G, Lin H (2016) Green Chem 18:2726
26. Wang L, Xu G, Xiao J (2019) Ind Eng Chem Res 58:12401
27. Xu G, Wang L, Li M (2017) Green Chem 19:5818
28. Du J, Shuai B, Tao M (2016) Green Chem 18:2625
29. Ma L, Yuan L, Xu C (2012) Synthesis 45:45
30. Li P, Liu Y, Ma N (2018) Catal Lett 148:813
31. Shi XL, Chen Y, Hu Q (2018) Ind Eng Chem Res 57:7450
32. Xu G, Cao J, Zhao Y (2017) Chem Asian J 12:2565
33. Zheng L, Li P, Tao M (2019) Catal Commun 118:19
34. Li P, Liu Y, Cao J (2017) ChemCatChem 9:3725
35. Love D, Kim K, Domaille DW (2019) Polym Chem 10:5790
36. Amara Z, Caron J, Joseph D (2013) Nat Prod Rep 30:1211
37. Wang J, Li P, Choy PY (2012) ChemCatChem 4:917
38. Mahe O, Dez I, Levacher V (2010) Angew Chem Int Ed 49:7072
39. Ghasemi MH, Kowsari E, Shafiee A (2016) Tetrahedron Lett 57:1150
40. Ghasemi MH, Kowsari E (2016) Res Chem Intermed 43:3691
41. Zussman E, Chen X, Ding W (2005) Carbon 43:2175

42. Geng Z, Zhang H, Xiong Q (2015) J Mater Chem A 3:19455
43. Qin H, Gong T, Cho Y (2014) Polym Chem 5:4466
44. Roy SR, Chakraborti AK (2010) Org Lett 12:3866
45. Ying A, Li Z, Yang J (2014) J Org Chem 79:6510
46. Song Y, Cheng C, Jing H (2014) Chem Eur J 20:12894
47. Lan DH, Gong YX, Tan NY (2018) Carbon 127:245